University of

HUDDERSFIELD

University of Huddersfield Repository

Greaves, Graeme, Hinks, J. A., Busby, P., Mellors, N. J., Ilinov, A., Kuronen, A., Nordlund, K. and Donnelly, S. E.

Enhanced Sputtering Yields from Single-Ion Impacts on Gold Nanorods

Original Citation

This version is available at http://eprints.hud.ac.uk/18151/

http://eprints.hud.ac.uk/

Enhanced Sputtering Yields from Single-Ion Impacts on Gold Nanorods

G. Greaves[1], J. A. Hinks[1], P. Busby[2], N. J. Mellors[2], A. Ilinov[3], A. Kuronen[3]
K. Nordlund[3] and S. E. Donnelly[1]

[1]*School of Computing and Engineering, University of Huddersfield,
Huddersfield HD1 3DH, UK*

[2]*School of Computing, Science and Engineering, University of Salford,
Manchester M5 4WT, UK*

[3]*Department of Physics, University of Helsinki, P.O. Box 43,
Helsinki FI–00014, Finland*

Sputtering yields, enhanced by more than an order of magnitude, have been observed for 80 keV Xe ion irradiation of monocrystalline Au nanorods. Yields are in the range 100–1900 atoms/ion compared with values for a flat surface of $\approx$ 50. This enhancement results in part from the proximity of collision cascades and ensuing thermal spikes to the nanorod surfaces. Molecular dynamic modeling reveals that the range of incident angles occurring for irradiation of nanorods and the larger number of atoms in "explosively ejected" atomic clusters make a significant contribution to the enhanced yield.

PACS numbers: 61.05.J-, 61.46.Km, 61.80.Jh, 61.80.Az

Flow processes resulting from single, heavy-ion impacts on flat surfaces of dense metals cause changes in surface topography involving the displacement of tens of thousands of atoms and resulting in features such as craters and protrusions with dimensions on the order of 10 nm [1–3]. Such processes have been observed primarily on Au surfaces but also for Ag, In and Pb [4]. They occur where the mean free path between successive collisions, in the collision cascade resulting from the ion impact, is on the order of an atomic spacing. Under these conditions, the binary collision approximation [5], generally used successfully to model collision processes, may no longer be fully applicable and the energy dissipation may be better approximated by an energy- or thermal-spike model [6]. As the spike size is typically several nanometers, ion irradiation of nanostructures may yield enhancement of effects resulting from cascade interaction with the surface [7].

In this Letter we report on an *in-situ* Transmission Electron Microscopy (TEM) study of Au nanorods under irradiation, at room temperature, with 80 keV Xe^+ ions. Using volume calculations based on TEM image measurements, we have determined sputtering yields, *S*, and have obtained values more than an order of magnitude larger than those for similar irradiations of flat Au surfaces. Estimations have been made of the maximum contribution to *S* expected from ballistic ejection and evaporative loss of material during the thermal spike. Although this yields an enhancement to *S* of a factor of about four over that for flat surfaces, it fails to account for the values measured. Molecular dynamics (MD) simulations reveal that a combination of varied angles of incidence and "explosive" ejection of nanoclusters by the thermal spike can contribute to the increased yield which may be further enhanced by the proximity of cascades to the surface.

Au nanowires were fabricated by electrodeposition into an anodic Al_2O_3 template with 20 nm diameter pores. The template was then dissolved in 0.1 M NaOH and the resulting nanowires rinsed in distilled water and deposited onto holey-Formvar-coated Cu TEM grids. Electron microscopy and diffraction indicated that the nanowires were approximately 20 nm in diameter, microns in length and consisted of columnar grains on the order of 100 nm in length with no preferred growth direction.

Specimens were irradiated at room temperature in a JEOL 2000FX TEM operating at 200 kV in the MIAMI facility at the University of Huddersfield [8]. The ion flux was $2.1\pm0.1 \times 10^{11}$ ions cm^{-2} s^{-1} with measurements made periodically during experiments by

translating a Faraday cup into the specimen position. The fluence range over which volume measurements were made was 0.0–7.0 × 10^{13} ions cm^{-2}.

The TEM grids were horizontal in the microscope with the ion beam incident on the specimen at 30° from the electron beam. The angle between the ion beam and the axis of the nanorod was variable. Video (480 × 480 pixels at 8 frames per second) was captured using a Gatan SC200 digital camera.

Following irradiation to an initial fluence of approximately 2.1 × 10^{14} ions cm^{-2}, the nanowires separate at grain boundaries into nanorods as a result of flow and sputtering processes. FIG. 1a shows a nanowire fragmented into nanorods. The small particles surrounding the nanorods result from sputter-deposition of Au onto the Formvar film, causing the growth of nanoparticles.
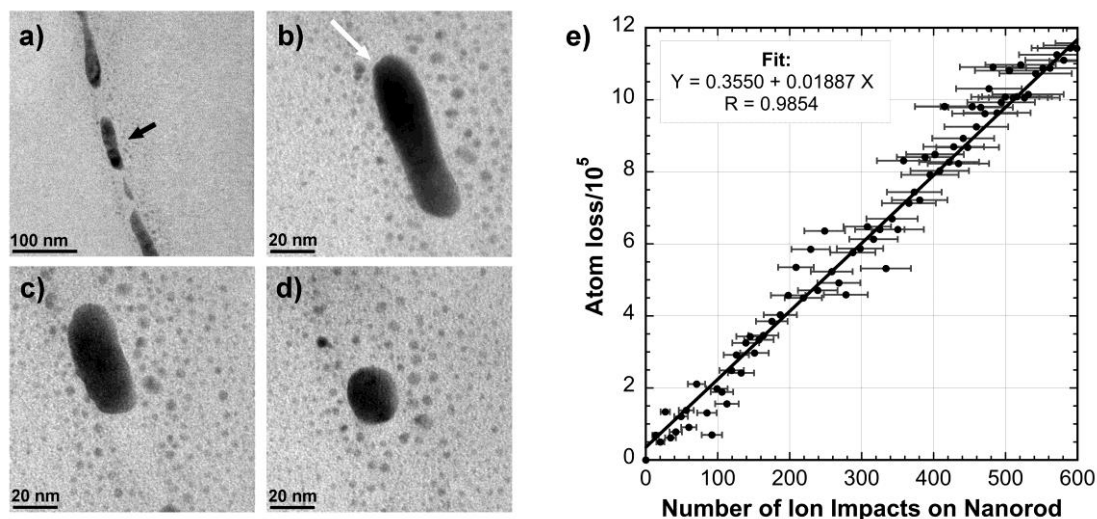

FIG 1. Changes to Au nanowire due to irradiation with 80 keV Xe ions. a) segmentation due to "necking" and breaking of nanowire at grain boundaries following irradiation to a fluence of 2.1 × 10^{14} ions cm^{-2}; b) nanorod at starting point for volume measurements – white arrow indicates projected direction of the ion beam which was incident at 60° to the specimen plane; c) nanorod following irradiation to (additional) fluence of 1.6 × 10^{13} ions cm^{-2} (≈ 227 impacts on nanorod) d) nanorod following irradiation to (additional) fluence of 5.5 × 10^{13} ions cm^{-2} (≈ 316 additional impacts on nanorod). All are bright field TEM images. e) Plot of atom loss versus ion impacts for Au nanorod shown in panels b) to d).

Diffraction contrast is always observed in the nanorods; as in the case for heavy ion irradiation of Au foils, the Au remains solid during irradiation. Changes to the rods result from loss of atoms by sputtering and redistribution of atoms by flow [1–4].

In two experiments, images, recorded at tilts from 0–100° in 10° steps about the axis of the individual nanorods, confirmed that their cylindrical symmetry was retained during the experiments.

S was determined for isolated nanorods, with an example shown in FIG. 1b. FIGs. 1 c) and d) illustrate the changes observed during the experiment. The volume V was determined at fluence intervals of 4.0 × 10^{11} ions cm^{-2} by measuring the radius, r_i, of the nanorod at small increments, Δx_i (2 pixels = 0.46 nm), along its axis and calculating, over the length of the rod, the sum:

$$V = \sum_i \rho r_i^2 \mathrm{D} x_i \qquad \text{................. (1)}$$

The number of impacts on the nanorod was calculated from the fluence and projected area of the nanorod, with a trigonometric correction for the angle between electron and ion beams.

FIG. 1e shows data for a nanorod for which S was determined to be 1887±207 atoms/ion. Experiments have been conducted on an additional 4 nanorods for which S was 823±85, 1036±87, 175±21 and 147±12 atoms/ion. In three experiments, S is significantly enhanced compared to the value for 80 keV Xe ions on planar Au surfaces of approximately 50 [9]

although this figure could be 3 or more times higher for non-normal incidence [10]. In two cases there is a smaller enhancement. Although the orientation of the ion beam with respect to crystallographic directions in the nanowire was not generally measured, in the case of the nanowire with a measured S of 147, diffraction analysis revealed that the ion beam was aligned with a <112> direction (±2°). This will be discussed further below.

The proximity of the collision cascade to the surface of the nanorod will result in some enhancement in S due to ballistic and evaporative processes which we estimate below.

Ballistic sputtering: Sputtering will occur in the ballistic phase of the cascade due to its intersection with the surface, with atoms at the surface having sufficient kinetic energy and appropriately oriented momentum to be ejected. The Monte-Carlo code SRIM [11] has been used to analyze the energy-deposition distribution resulting from 100 individual collisions of Xe ions with a planar Au surface. A clear (unsurprising) correlation is obtained between the amount of energy deposited in nuclear collisions in a 1 nm layer below the surface and the calculated sputtering yield. This relation, together with the energy-deposition profile due to individual cascades calculated from the SRIM code has been used to estimate the ballistic component, S_B, for a 20 nm Au cylinder due to 100 individual impacts. This yields a value of S_B for the nanorod of 105 ($\approx$ 4 times the value of 26 calculated for flat surfaces).

Evaporative sputtering: For an isotropic solid in which thermal energy, E, is deposited as a point source at a position $r = 0$ at a time $t = 0$, at any subsequent time, t, the temperature, T, at a distance, r, is given by [12]:

$$T = T_0 + \frac{1}{Nk} \frac{E}{(4\rho Dt)^{3/2}} \exp\left(\frac{-r^2}{4Dt}\right) \quad \text{.................... (2)}$$

where T_0 is the initial temperature, N is the atomic density of the solid, k is Boltzmann's constant and D is the thermal diffusivity.

We approximate the thermal spike to a spherically symmetrical volume with the initial temperature distribution following a radial Gaussian spatial profile. Eqn. 2 can then be used to describe its temperature evolution by making the substitution: $t = t' + t_0$, where t_0 is the time at which the temperature profile resulting from the point source exactly matches that of the thermal spike and t' is the elapsed time from the moment of the ion impact (neglecting the sub-picosecond ballistic phase of the collision cascade).

T at any point within the nanorod at time t' can thus be calculated provided that the position of the center of the spike and the deposited energy, E, are known. By calculating T at a point on the surface, the evaporation rate, a, from this point can be obtained from:

$$a = N\sqrt{\frac{kT}{2\rho M}} \exp\left(\frac{-U}{kT}\right) \quad \text{..............................(3)}$$

where M is the mass of an Au atom and U is the energy input required for evaporation [13]. By making the maximizing assumption that all heat loss at the surface is due to evaporation, an upper limit to the evaporation due to spikes centered on locations representative of the cascade distribution (as calculated using the SRIM code) can be determined. By integrating a over the lifetime of each spike and the surface area of the nanorod, the evaporative component, S_E, of S can be estimated. Note that, given the short lifetime of the spike, there is minimal coupling of the deposited energy into the electronic system. The appropriate value of D is, thus, one typical of insulators and we have used a value of 10^{-6} m^2 s^{-1} which is approximately 100 times smaller than the equilibrium value for Au and similar to values for alumina and silica. This calculation yields $S_E = 122$; approximately 3.5 times the value of 35 similarly calculated for a flat Au surface. (The thermal spike lifetime from our calculations is $\approx$ 15 ps as also obtained by Averback in MD simulations of 10 keV Au impacts on Au [14].) Summing the two components yields a value for $S = S_B + S_E = 227$. This represents an approximately fourfold enhancement of the similarly calculated value for a flat surface of $S = 61$. This latter value is somewhat larger than $S \approx$ 50 extrapolated from a compilation of experimental data by Andersen and Bay [9].

In order to gain an understanding of processes not included in the simple considerations

*Published in Phys. Rev. Letters **111** (2013) 065504 (8 August 2013)*

3

above, MD simulations of 80 keV Xe impacts were performed on an Au nanorod 70 nm in length and 20 nm in diameter (50 nm cylinder with hemispherical ends). Details of our MD simulations of ion impacts on Au and our general simulation principles have been reported previously [15,16]. Au interactions were modeled using the embedded-atom method (EAM) potential by Foiles *et al*. [17]. This gives a good description of a range of Au properties [18], including surface irradiation effects [3,19,20,21]. For high-energy collisions we have used the universal Ziegler–Biersack–Littmark (ZBL) interatomic repulsive potential [11] that complements the EAM potential at small interatomic distances. ZBL electronic stopping was applied for all atoms with a kinetic energy $\geq$ 5 eV [22,23].

The upper plane of the nanorod was a (100) surface and ions were fired from random positions above the rod. The angles between the nanorod axis and the ion trajectories were selected randomly in the range 90°±20°. After each irradiation, the system was simulated for 200 ps without any temperature control, after which the rod was cooled to 300 K to mimic the experimental situation of cooling via thermal conduction through the Formvar film. Using black-body radiation theory we calculated that radiative cooling can be neglected.
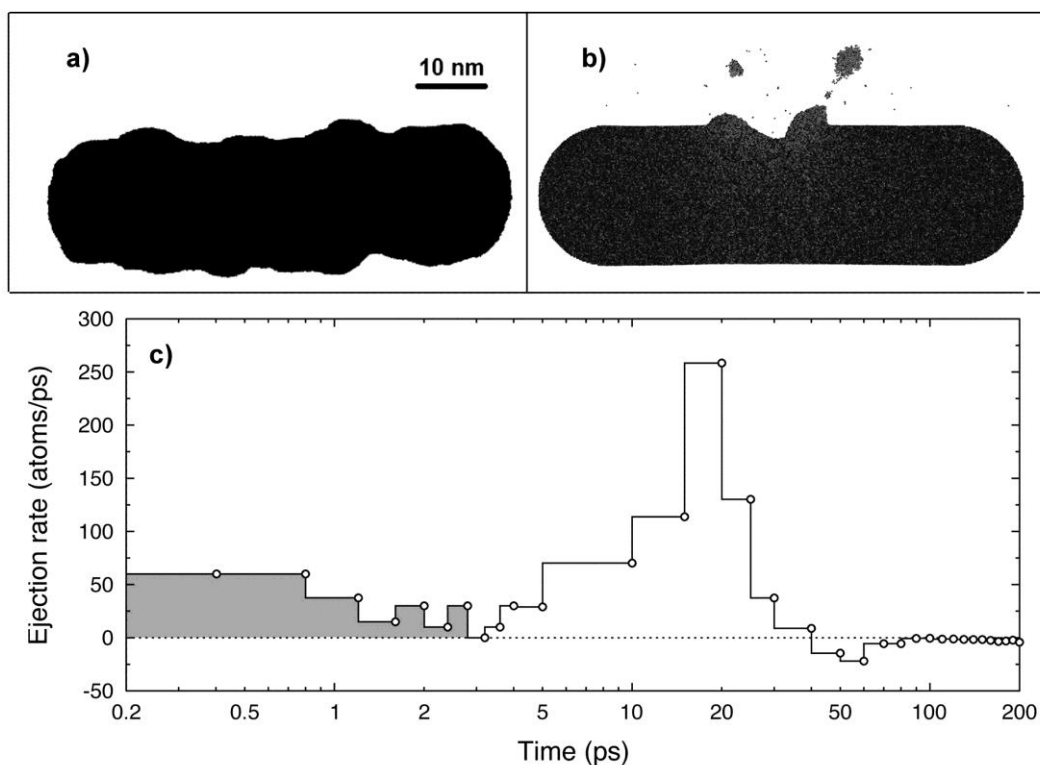

FIG. 2: Results of MD simulations of 80 keV Xe ions on an Au nanorod: a) silhouette of the nanorod following 30 impacts; b) image at 80 ps following a single impact showing a crater and ejected nanoclusters; c) plot of ejection rate (atoms/ps) as a function of time for a single 80 keV Xe ion impact. The shaded area indicates the contribution from ballistic and evaporative processes. Each point indicates the mean ejection rate for the period since the previous point. The negative ejection values around 50 ps result from atoms evaporated from the clusters being redeposited on the nanorod (cf. Ref. [21]).

In FIG. 2b a crater and expelled material from sputtering and localized flow processes are visible. It should be noted, however, that craters observed to form in our experiments are generally seen to disappear due to flow events from local ion impacts [2]. Such events are less prevalent in simulations, partially due to the small number of ions simulated.

FIG. 2b illustrates an important process not considered in standard models of sputtering which appears to be partially responsible for the enhanced sputtering yields: cluster emission. In this image, two clusters have been "explosively" ejected by the spike. FIG. 2c is a plot of ejection rate versus time for the impact in FIG 2b indicating that, for this event, the sputtering yield is dominated by the cluster contribution. Specifically, the contribution from "normal"

ballistic and evaporative processes is $\approx$ 100 out of a total S of 2560. Clusters containing $\geq$ 100 atoms occur in 60% of the 30 collisions that we have simulated where the ion is not incident along a channeling direction. In our set of 30 simulated impacts, S varied from 20 to 3159 with a mean of 1005±182. When the incident Xe ion direction was well aligned with a channel, S reduced to near zero as the ion channeled with only a small loss of energy.

To explore the effect of the angle of incidence, we have simulated 20 impacts for a bulk Au sample for each of seven angles (normal to glancing) and weighted these data appropriately for the nanorod shape and the experimental geometry. This yields a significantly increased value of $S = 388\pm89$ – but this is much less than the average value from MD simulations of 1005. Exit sputtering due to ions incident at grazing incidence at the outside of the nanorods may also contribute to the enhanced yield – and overall, this discrepancy indicates that nanosize effects make an important contribution to the yield enhancement.

To estimate the importance of channeling, we performed range calculations of 80 keV Xe on Au single crystals of different orientations using the MDRANGE code [23], previously shown to give a good description of ion ranges in crystal channels [24,25]. Au atoms were arranged in perfect crystals with random thermal displacements, based on the Debye model, corresponding to 300 K with a Debye temperature of 170 K [26]. The surface normal was in the <100>, <110> , <111> or <112> crystal direction and the twist (φ) angle was chosen randomly. ZBL electronic stopping [11] was applied to the ion. The simulations showed the half-angle for channeling for 80 keV Xe on Au to be between 3° and 5° for the four directions. Similarly wide channels have also been observed in experiments [27]. Mean ranges were enhanced by factors of 4–10 and, specifically in the <112> direction, the mean range was 53±3 nm compared with 12.2±0.2 nm in a non-channeling direction. With a mean range more than twice the nanorod width, it is likely that the channeled ions will deposit little energy in the nanorod.

Given the wide half-angle for channeling and the possibility of both axial and planar channeling with concomitant reduction of energy loss in the nanorods, differing degrees of channeling are a likely explanation for the range of values for S observed in our experiments. Further work is underway to quantify this effect.

A combination of factors including surface proximity, varied angles of incidence and the "explosive" emission of atomic clusters is responsible for a significant enhancement of sputtering yields for heavy ion impacts on Au nanorods over those for flat surfaces. Although simulations reveal that clusters are also emitted from flat surfaces these are smaller and fewer. These factors will also apply, to varying degrees, for heavy-ion collisions on other types of nanostructure involving dense materials and will need to be taken into account when using ion beams to process nanostructures.

[1] R. C. Birtcher, S. E. Donnelly, Phys. Rev. Lett. **77** (21) 4374 (1996).
[2] S. E. Donnelly, R. C. Birtcher Phys. Rev. B **56** (21) 13599 (1997).
[3] K. Nordlund , J. Tarus, J. Keinonen , S. E. Donnelly, R.C. Birtcher, Nucl. Instrum. Meth. B **206** 189 (2001).
[4] S. E. Donnelly, R. C. Birtcher, Philos. Mag. A **79**(1) 133-145 (1999).
[5] M.T. Robinson, I. M. Phys. Rev. B **9** 5008 (1974).
[6] J. A. Brinkman, J. Appl. Phys. **25** (8) 961 (1954).
[7] T. T. Järvi, J. A. Pakarinen, A. Kuronen, K. Nordlund, Europhys. Lett. **82** 26002 (2008).
[8] J. A. Hinks, J. A. van den Berg, S. E. Donnelly, J. Vac. Sci & Technol. A **29**(2) 021003 (2011)
[9] H. H. Andersen, H. L. Bay, in *Sputtering by Particle Bombardment I* (Topics in Applied Physics **47**), R. Behrisch (Ed), 145, Springer Berlin Heidelberg (1981).
[10] J. M. Fluit, P. K. Rol, and J. Kistemaker, J. Appl. Phys. **34**, 690 (1963).
[11] J.F. Ziegler, J.P. Biersack, U. Littmark, The Stopping and Range of Ions Matter, Pergamon, New York, USA, (1985).
[12] H. S. Carslaw and J. C. Jaeger, *Conduction of Heat in Solids* (Clarendon Press, Oxford, 1959), p. 256.

[13] P Sigmund, Ref [9] 9.

[14] R. S. Averback, J. Nuc. Mater **216** 49 (1994).

[15] J. Samela, K. Nordlund, Nucl. Instrum. Meth. **B** 263 375 (2007)

[16] K. Nordlund, M. Ghaly, R. S. Averback, M. Caturla, T. Diaz de la Rubia, J. Tarus, Phys. Rev. B, **57**(13) 7556 (1998).

[17] S. M. Foiles, M. I. Baskes, and M. S. Daw, Phys. Rev. B, 33(12) 7983 (1986). Erratum: ibid, Phys. Rev. B **37** 10378 (1988).

[18] M. S. Daw, S. M. Foiles, M. I. Baskes. Mat. Sci. Rep. **9** 251 (1993)

[19] J. Samela, J. Kotakoski, K. Nordlund, J. Keinonen, Nucl. Instr. and Meth. B **239** 331 (2005).

[20] M Ghaly, R. S. Averback. Phys. Rev. Lett., **72**(3) 364 (1994)

[21] K.O.E. Henriksson, K. Nordlund, J. Keinonen, Phys. Rev. B **71** 014117 (2005)

[22] K. O. E. Henriksson, K. Nordlund, and J. Keinonen. Nucl. Instr. Meth. B **255**(1) 259 (2007)

[23] K. Nordlund. Comput. Mater. Sci. **3** 448, (1995).

[24] J. Sillanpää, K. Nordlund, J. Keinonen, Phys. Rev. B, **62** 3109 (2000).

[25] J. Peltola, K. Nordlund, J. Keinonen. Nucl. Instr. Meth. B, **212** 118 (2003).

[26] N. W. Ashcroft and N. D. Mermin, *Solid State Physics*, (Saunders College, Philadelphia,1976).

[27] J. Nord, K. Nordlund, B. Pipeleers, and A. Vantomme. Mater. Sci. & Eng. B,**105**(1) 110 (2003).